Supplemental Information for:

Molecular Analysis of pSK1 *par*: A Novel Plasmid Partitioning System Encoded by Staphylococcal Multiresistance Plasmids

Helena Y. Chan[1], Slade O. Jensen[2-3], Rebecca J. LeBard[1#], William A. Figgett[1##], Evelyn Lai[1], Alice E. Simpson[1], Anthony J. Brzoska[1], Danielle S. Davies[1], Angela M. Connolly[1], Stuart J. Cordwell[1], Brady A. Travis[4], Raul Salinas[4], Ronald A. Skurray[1], Neville Firth[1], Maria A. Schumacher[4,*]

[1]School of Life and Environmental Sciences, University of Sydney, New South Wales 2006, Australia

[2]Microbiology and Infectious Diseases, School of Medicine, Western Sydney University, New South Wales 2751, Australia

[3]Antibiotic Resistance & Mobile Elements Group, Ingham Institute for Applied Medical Research, New South Wales 2170, Australia

[4]Department of Biochemistry, Duke University School of Medicine, Durham NC 27710, USA

#Current address: School of Biotechnology & Biomolecular Sciences, University of New South Wales, Sydney, New South Wales, Australia

##Current address: Garvan Institute of Medical Research, 384 Victoria St, Darlinghurst, New South Wales, 2010, Australia

***Correspondence:** Maria.schumacher@duke.edu

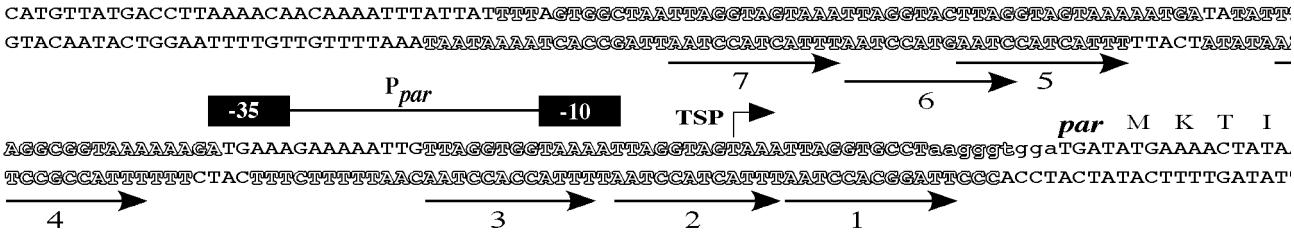

Figure S1. Sequence of the *par* upstream intergenic region. The DNA segment shown corresponds to nucleotides 1892-1713 of the pSK1 plasmid (GenBank entry GU565967). Black boxes represent –10 and –35 sequences of the *par* promoter, P_{par}. The nucleotides protected by Par from DNase I digestion are shown in outline text and the numbered arrows in this region indicate centromere-like repeat elements. The *par* transcriptional start point (TSP) is indicated by a bent arrow, and the *par* ribosome binding site is shown in lower case.

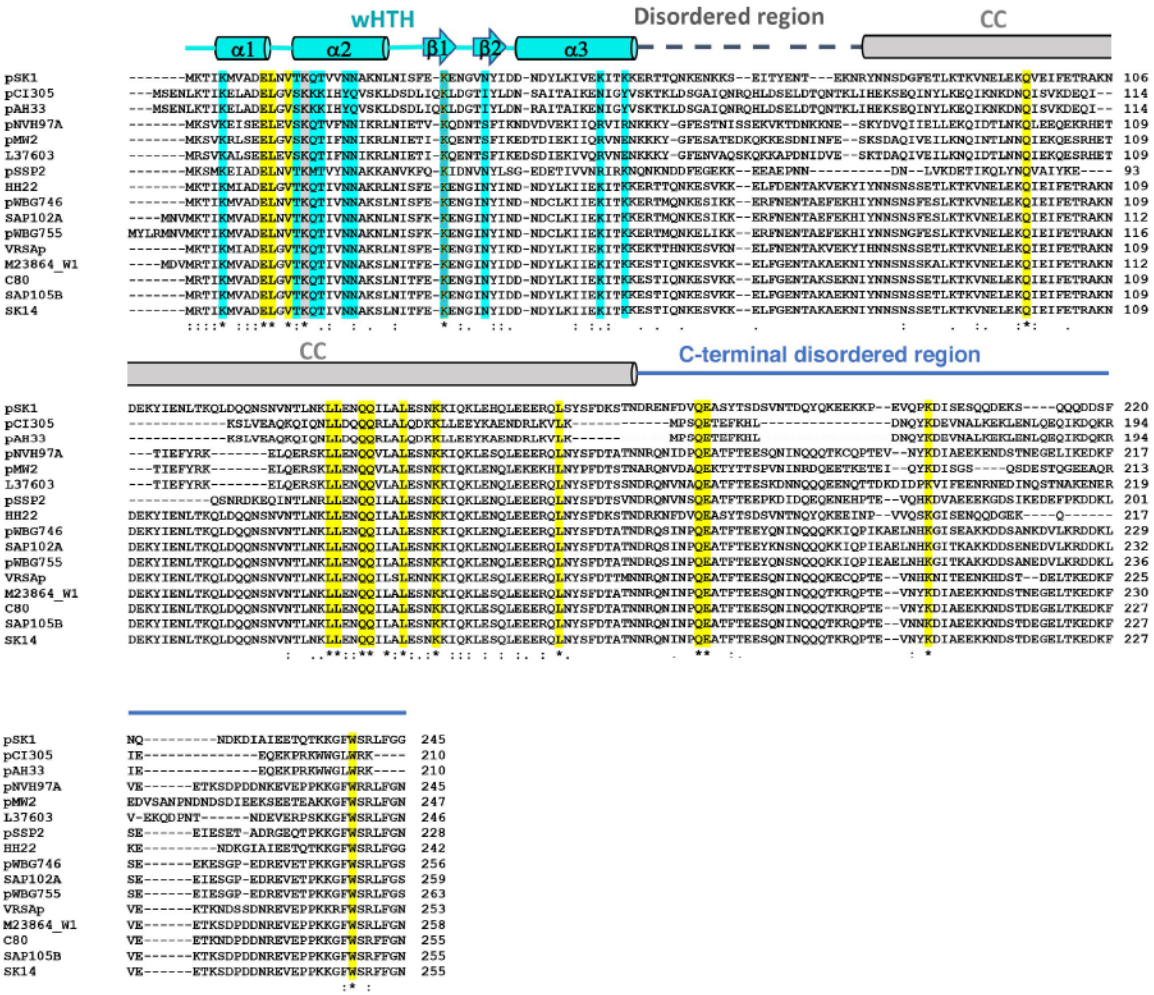

Figure S2. Sequence alignment of pSK1 Par homologs. The regions of the protein are labeled over the sequence, including the winged helix-turn-helix (wHTH), disordered region (that is subject to proteolysis), the putative coiled coil (CC) and the C-terminal disordered region. The secondary structural elements revealed in the crystal structure are shown within the wHTH. Invariant, conserved and somewhat conserved residues are indicated by asterisks, double circles and single circles, respectively, under the sequence. Residues in the wHTH that contact DNA are colored cyan (as a subunit in Figure 3A) except Lys15 which is colored grey. Invariant residues outside those contacting DNA are colored yellow.

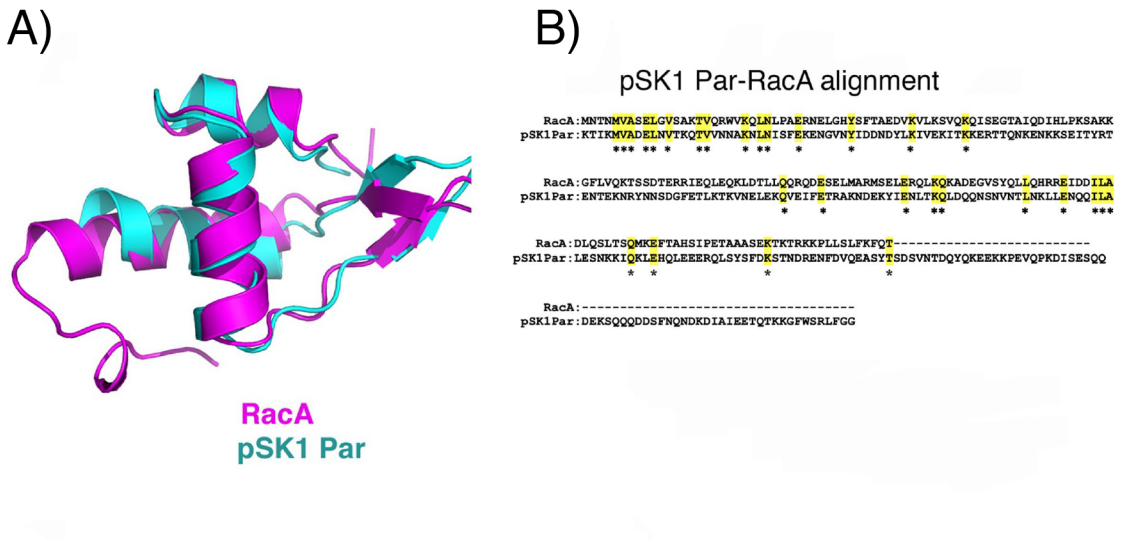

Figure S3. The structure of the pSK1 Par DNA-binding domain shows homology to the structure of the *B. subtilis* RacA DNA-binding domain. **(A)** Superimpositions of pSK1 Par DNA-binding domain onto that of RacA and (**B**) Sequence alignment of RacA and pSK1 Par.

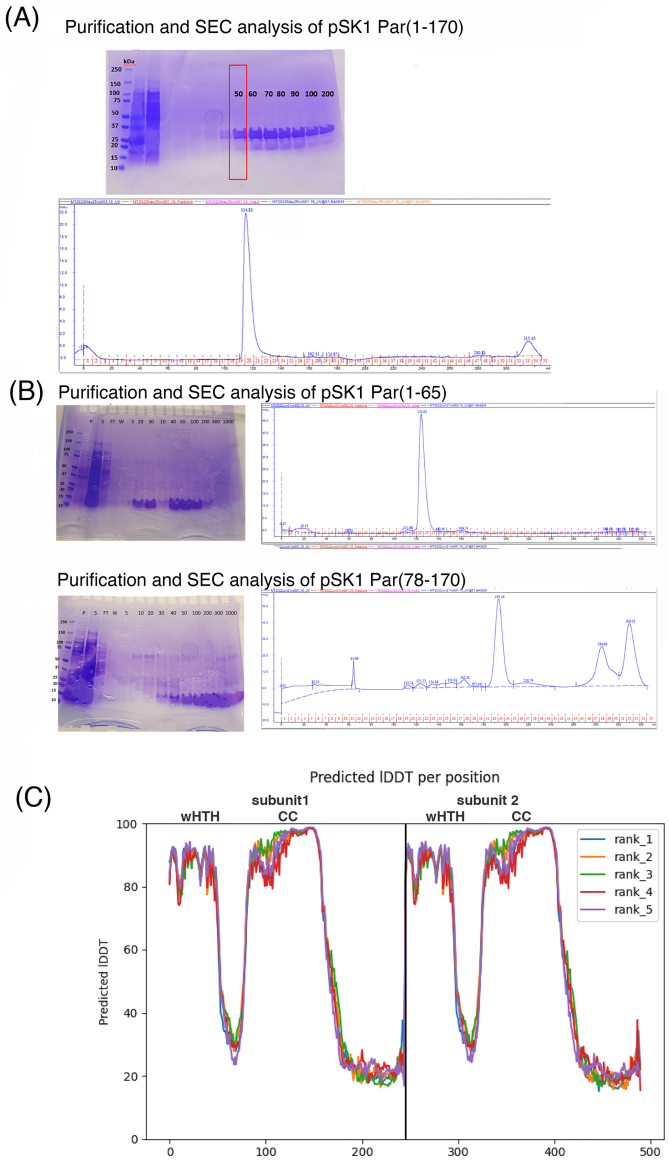

Figure S4. pSK1 Par oligomerization. (**A)** Purification and SEC analysis of pSK1 Par(1-170). SDS page shows purity of the protein, the band highlighted was used for SEC with an S75 column (Materials and methods). Based on calibration of standards the estimated MW is 90 kDa, which is most consistent with a dimer-of-dimer or tetramer. (**B**) Purification and SEC analysis of pSK1 Par(1-65) and Par(78-170). SDS page gels shows the purity of the proteins. SEC analyses provided estimated MWs of 65 and 12 kDa, respectively which is consistent with a monomeric wHTH (Par(1-65) and dimer-of-dimer or tetramer for pSK1 Par(78-170) (Note all these proteins contain a 20 residue N-terminal tag, which includes a His_6 tag). The MW of the latter may be higher due to shape (non-globular proteins exhibit larger MW than the globular equivalent). (**C**) Output from Alphafold 2 run with pSK1 Par (sequences linked to observe possible dimer prediction). Note residues 1-50 (labeled “wHTH”) and 78-180 (labeled “CC”) are predicted with high reliability (pLDDT >90%) for the two subunits of the dimer. The x and y axis indicate the Predicted lDDT and residue number (where subunit 2 is numbered consecutively after subunit 1 due to the linkage). Rank refers to the 5 models that were output in the run. Note all runs produced similar results and structures for the reliably predicted domains.

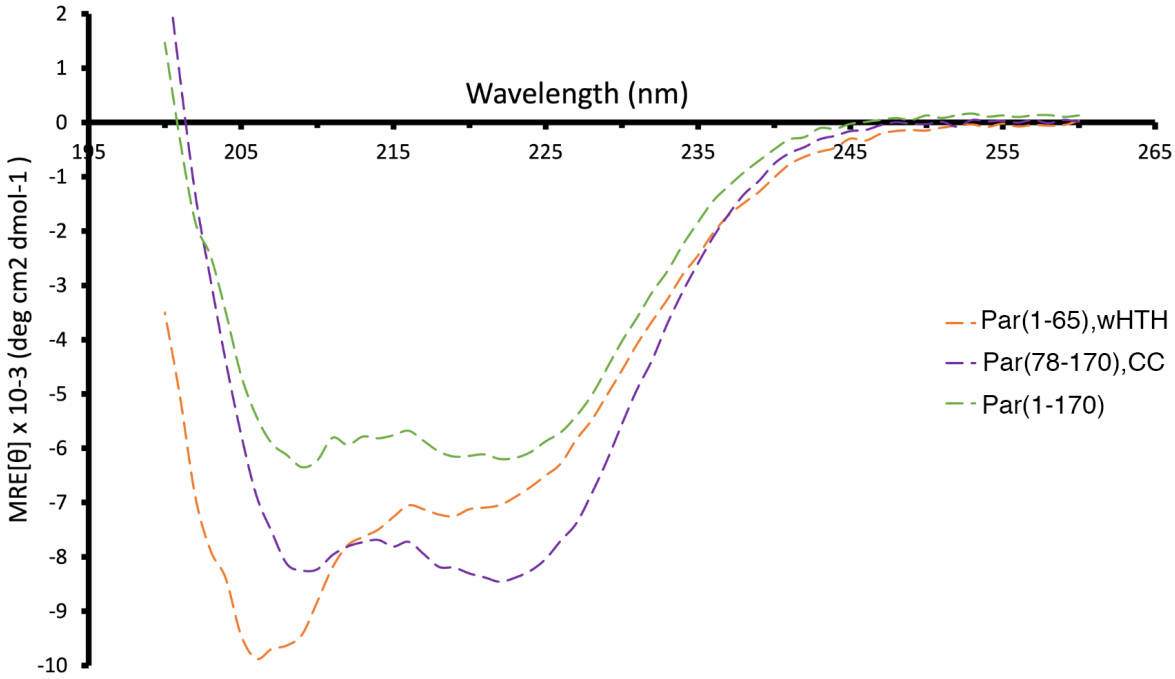

Figure S5. Far-UV CD spectra of pSK1 Par(1-170), pSK1 Par(1-65), and pSK1 Par(78-170). The samples were in a buffer consisting of 20 mM NaH_2PO_4 (pH 7.5), 300 mM NaF, 5% glycerol, and 1 mM TCEP.

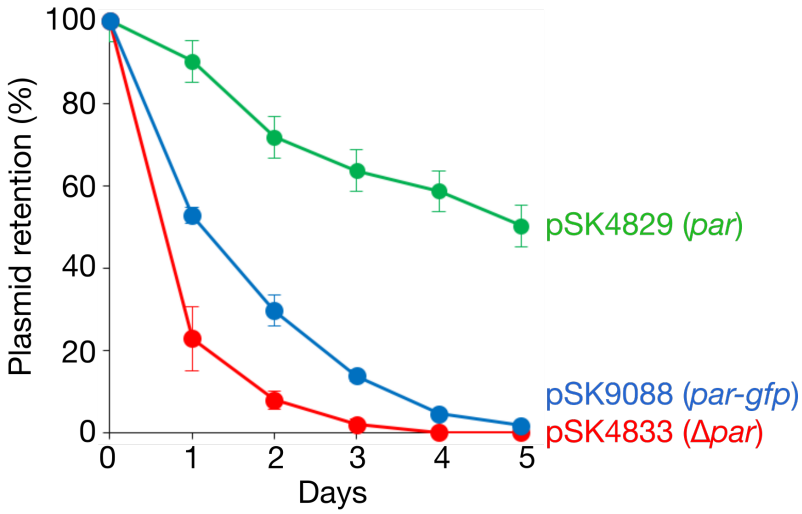

Figure S6. Plasmid segregational stability assay of a pSK1 minireplicon encoding Par-GFP in *S. aureus*. The retention of pSK1 minireplicons pSK4829 (*par*, green), pSK4833 (Δ*par*, red) and pSK9088 (P_{par}::*par-gfp*, blue) was determined for five days of serial subculture (~75 generations) in the absence of selection. Each data point is the mean of three independent assays, each normalized to 100% plasmid retention on Day 0. Error bars indicate standard error of the mean.

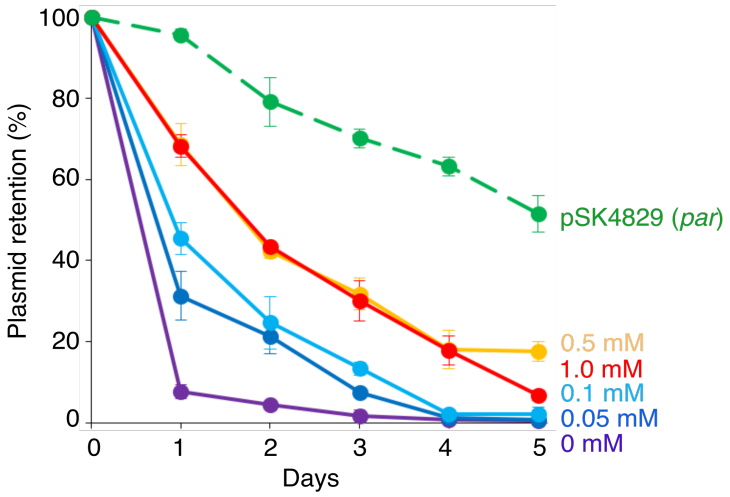

Figure S7. Segregational stability of pSK1 minireplicon pSK4833 (Δ*par*) in the presence of untagged Par, provided *in trans* from pSK9104 (P_{spac}::*par*), induced with 0 mM (purple), 0.05 mM (dark blue), 0.1 mM (light blue), 0.5 mM (orange) or 1.0 mM (red) IPTG. Cells were subcultured for five days (~75 generations) in the presence of tetracycline (to maintain selection for pSK9104) and the appropriate concentration of IPTG. The segregational stability of pSK4829 is included as a reference. Each data point is the mean of three independent assays, each normalized to 100% plasmid retention on Day 0. Error bars indicate standard error of the mean.

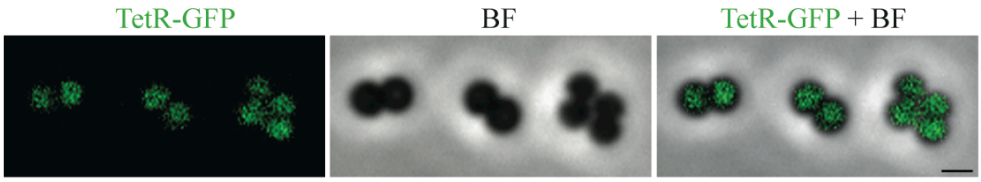

Figure S8. Fluorescence localization of TetR-GFP in the absence of *tet*O arrays. TetR-GFP expression was induced from pSK9142 (P_{spac}::*tetR-gfp*) with 0.1 mM IPTG in *S. aureus* cells harboring a pSK1 minireplicon lacking *tet*O arrays (pSK4829, *par*). From left to right: TetR-GFP, bright-field (BF), and merge of TetR-GFP and BF channels. Scale bar = 1 µm.

Table S1. Bacterial strains, plasmids and oligonucleotides

Strain, plasmid or oligonucleotide	Genotype, relevant characteristics or sequence [a]	Reference or source
E. coli		
DH5α	F- *endA hsdR17 supE44 thi-1 λ- recA1 gyrA96 relA1* ϕ80 *dLacZ*ΔM15	Bethesda Research Laboratories
M15	F- *thi- lac- ara+ gal+ mtl- recA+ uvr+ lon+*	Qiagen
C41(DE3)	F- *ompT hsdSB (rB- mB-) gal dcm*	(6)
S. aureus		
RN4220	Restrictionless derivative of NCTC 8325–4	(7)
Plasmids		
pJEG015	Ap^R, Tc^R, pLOW-GFP with *ermC* replaced by *tetA(K)*	This study
pLAU44	Ap^R, Gm^R, pUC18 carrying an array of 120 copies of the 19-bp Tn10 *tet*O binding site separated by 10-bp random spacer sequence, flanking either side of a gentamicin resistance gene	(8)
pLOW-GFP	Ap^R, Em^R, *E. coli–S. aureus* shuttle plasmid containing IPTG-inducible P_{spac} promoter and *lacI* for controlled expression of *gfp* fusions in *S. aureus*	(9)
pQE-30	Ap^R, *E. coli* expression vector containing IPTG-inducible T5 promoter and *lac* operator	Qiagen
pRB394	Ap^R, Nm^R, pBR322 *ori*, pUB110 *ori*, MCS-promoterless *cat* gene from pUB112	(10)
pREP4	Km^R, *lac* repressor gene (*lacI*)	Qiagen
pSK1	*S. aureus* 28.2 kb multiresistance plasmid	(11)
pSK4829	Ap^R, Em^R, pSK1 *par-rep* coding region cloned into the *Bam*HI and *Hin*dIII sites of pWE180	(12)
pSK4833	Ap^R, Em^R, pSK1 *rep* coding region cloned into the *Bam*HI and *Hin*dIII sites of pWE180	(12)
pSK5336	Ap^R, Nm^R, pSK1 *par-rep* intergenic region cloned into the *Bam*HI and *Hin*dIII sites of pRB394	This study
pSK5344	Ap^R, pSK1 *par* coding region cloned into the *Bam*HI and *Hin*dIII sites of pQE-30	This study
pSK6133	Ap^R, Em^R, pSK4829 site-directed mutant; -10 region of P_{mal} changed to a *Sma*I site (see Figure 1A)	This study
pSK6134	Ap^R, Nm^R, pSK5336 site-directed mutant; -10 region of P_{mal} changed to a *Sma*I site (see Figure 1A)	This study
pSK6137	Ap^R, Em^R, pSK4829 site-directed mutant; -10 region of $P_{par\text{-}1}$ changed to a *Sma*I site (see Figure 1A)	This study
pSK6138	Ap^R, Nm^R, pSK5336 site-directed mutant; -10 region of $P_{par\text{-}1}$ changed to a *Sma*I site (see Figure 1A)	This study
pSK6144	Ap^R, Nm^R, pSK1 *par* coding region and the upstream direct repeats cloned into the *Eco*RI and *Bam*HI sites of pRB394	This study
pSK6147	Ap^R, Em^R, pSK4829 site-directed mutant; -10 region of $P_{par\text{-}2}$ changed to a *Mlu*I site (see Figure 1A)	This study
pSK6148	Ap^R, Em^R, pSK4829 site-directed mutant; -10 region of $P_{par\text{-}3}$ changed to a *Kpn*I site (see Figure 1A)	This study
pSK6149	Ap^R, Nm^R, pSK5336 site-directed mutant; -10 region of $P_{par\text{-}2}$ changed to a *Mlu*I site (see Figure 1A)	This study
pSK6150	Ap^R, Nm^R, pSK5336 site-directed mutant; -10 region of $P_{par\text{-}3}$ changed to a *Kpn*I site (see Figure 1A)	This study
pSK6152	Ap^R, Nm^R, pSK6144 site-directed mutant; two stop codons (TAA and TGA) were substituted at the second and fourth codon positions of *par*	This study
pSK7721	Ap^R, Em^R, pSK4829 site-directed mutant; *par* loop-out deletion nucleotides 247-465 (aa 83-155; ΔCC)	This study
pSK7728	Ap^R, pSK5344 site-directed mutant; *par* double point mutation TT395GC (L132A)	This study
pSK7764	Ap^R, Em^R, pSK4829 site-directed mutant; *par* double point mutation AA44GC (K15A)	This study
pSK7766	Ap^R, pSK5344 site-directed mutant; *par* double point mutation AA44GC (K15A)	This study
pSK7767	Ap^R, pSK5344 site-directed mutant; *par* loop-out deletion nucleotides 247-465 (aa 83-155; ΔCC)	This study
pSK9065	Ap^R, Nm^R, *E. coli–S. aureus* shuttle plasmid for controlled expression of *mRFPmars* fusions	(13)
pSK9067	Ap^R, Em^R, pLOW-GFP containing an additional $lacO_{id}$ operator upstream of P_{spac}	(13)
pSK9071	Ap^R, pSK5344 site-directed mutant; *par* C-terminal deletion of nucleotides 511-738 (aa 171-245; ΔCTD)	This study

pSK9088	Ap^R, Em^R, pSK1 *rep* and pSK1 *par-gfpmut-1* coding region cloned into the *Bam*HI and *Hin*dIII sites of pWE180. C-terminal Par-GFP fusion protein expressed from native pSK1 *par* promoter, P_{par}	This study
pSK9102	Ap^R, Tc^R, pSK1 *parK15A* and the native *par* RBS cloned into the *Sal*I and *Bam*HI sites of pJEG015 to generate a C-terminal *parK15A-gfp* fusion	This study
pSK9103	Ap^R, Tc^R, pSK1 *parΔCC* and the native *par* RBS cloned into the *Sal*I and *Bam*HI sites of pJEG015 to generate a C-terminal *parΔCC-gfp* fusion	This study
pSK9104	Ap^R, Tc^R, pSK1 *par* and the native *par* RBS, including stop codon, cloned into the *Sal*I and *Sma*I sites of pJEG015	This study
pSK9140	Ap^R, Nm^R, *aadD* gene cloned into the *Kpn*I and *Cla*I sites of pSK9067, replacing the *ermC* gene	This study
pSK9142	Ap^R, Nm^R, Tn*10 tetR* cloned into the *Sal*I and *Bam*HI sites of pSK9140	This study
pSK9144	Ap^R, Em^R, Tn*10 tet*O array cloned into the *Kas*I site of pSK4829	This study
pSK9145	Ap^R, Em^R, Tn*10 tet*O array cloned into the *Kas*I site of pSK4833	This study
pWE180	Ap^R, Em^R, pE194 erythromycin resistance gene (*ermC*) cloned into the blunted *Nde*I site of pUC18	(12)
Oligonucleotides[b]		
985*Eco*RI	5′-cgcgaattctcattagccaccaaacaaacgactccagaagcc-3′	This study
988*Hin*dIII	5′-gcgaagctttagccaccaaacaaacg-3′	This study
990*Bam*HI	5′-ttaaggatccagccaccaaacaaacgactcc-3′	This study
991*Hin*dIII	5′-gcgctgcagtcaagcttgccaccaaacaaacgactccagaagcc-3′	This study
994gfp	5′-catggaggcgccgcaggagccaccaaacaaacgactcc-3′	This study
1217ΔCTD*Hin*dIII	5′-gcgaagctttcatcgatcattagtagatttatc-3′	This study
1240ΔCC	5′-ggaataacttaattgtctctcgccatctgaattattatatctattcttttc-3′	This study
1310L132A	5′-gctaaaatttgttgattctct**gc**taatttatttaatgtattaac-3′	This study
1346L132A	5′-gttaatacattaaataaatta**gc**agagaatcaacaaatttttagc-3′	This study
1509ΔCC	5′-gaaaagaatagatataataattcagatggcgagagacaattaagttattcc-3′	This study
1661*Bam*HI	5′-gcgggatccgcattattaacaacagtttg-3′	This study
1661K15A	5′-gcattattaacaacagtttg**tgcag**ttacattcaattcatcag-3′	This study
1687*Eco*RI	5′-tacattcaattcatcagcaa**gaattctt****ca**agttt**a**catatcatccacccttag-3′	This study
1689	5′-cattcaattcatcagcaacc-3′	This study
1703K15A	5′-ctgatgaattgaatgtaac**tgcac**aaactgttgttaataatgc-3′	This study
1722*Bam*HI	5′-cgcggatccaaaactataaaaatggttgctgatg-3′	This study
1725*Eco*RI	5′-cgcgcgaattcatgaaaactataaaaatgg-3′	This study
1739*Sma*I	5′-ggcacctaatttactacct**acccggg**ccacctaacaatttttctttcatc-3′	This study
1740*Eco*RI	5′-ctaagggtggatgatatg**t**aaact**tg**aa**g**aa**ttc**ttgctgatgaattgaatgta-3′	This study
1743*Sal*I	5′-gattgtcgactgcctaagggtggatgatatg-3′	This study
1789*Sma*I	5′-gatgaaagaaaaattgttaggtgg**cccggg**taggtagtaaattaggtgcc-3′	This study
1797*Mlu*I	5′-ccgccta**acgcgt**tcatttttactacctaagtac-3′	This study
1830*Mlu*I	5′-gtacttaggtagtaaaaatga**acgcgt**taggcgg-3′	This study
1900	5′-atcagaatcatgttatgacc-3′	This study
1963*Kpn*I	5′-aagccaatgctatt**ggtacc**gcatcggctctggt-3′	This study
1996*Kpn*I	5′-accagagccgatgc**ggtac**caatagcattggctt-3′	This study
2037*Sma*I	5′-gcgttcgtttatttatatatttttttgatacttgt**cccggg**tatatctactcgtct-3′	This study
2066*Sma*I	5′-agacgagtagatata**cccggg**acaagtatcaaaaaaatatataaataaacgaacgc-3′	This study

2196*Hin*dIII	5′-gcgaagcttcgtaatgtttcgaattcacttgc-3′	This study
2727*Bam*HI	5′-gcgggatcctctcattcgaatcatacaaatcatc-3′	This study
3130*Bam*HI	5′-gcgggatcctttttctgttgacttaattcc-3′	This study
gfp_linker	5′-ggctcctgcggcgcctccatgagtaaaggagaagaac-3′	This study
gfp*Hin*dIII	5′-gcgaagctttttatttgtatagttcatcc-3′	This study
tetR*Sal*I	5′-cgcgtcgacttaggaggatgattatttatgtctagattagataaaagt-3′	This study
tetR*Bam*HI	5′-cgcggatcccggaggcgccgcaggaagacccactttcacattt-3′	This study
tetO*Kas*IF	5′-atcgcggcgccgctagcggccagtgccaagcttag-3′	This study
tetO*Kas*IR	5′-atcgcggcgccgctagcgtgatgcactttgatatcg-3′	This study

[a] Ap^R, ampicillin resistance; Em^R, erythromycin resistance; Gm^R, gentamicin resistance; Km^R, kanamycin resistance; LEU^+, leucine autotrophy; Nm^R, neomycin resistance; Tc^R, tetracycline resistance; TRP^+, tryptophan autotrophy. Nucleotide base substitutions are bolded and restriction sites are underlined. [b] The number refers to the 5' most base of each oligonucleotide that corresponds to pSK1 *par-rep* sequence (GenBank entry GU565967).

Table S2: Data collection and refinement statistics for pSK1 Par-DNA complex

Data	pSK1 Par-DNA/SAD	native pSK1 Par-DNA
Pdb code		8CSH
Space group	C2	C2
Cell constants (Å)	a=70.9, b=91.7,c=59.0	a=70.4, b=91.1, c=59.2
Cell angles (º)	$\alpha=\gamma=90.0$, $\beta=120.0$	$\alpha=\gamma=90.0$, $\beta=119.8$
Resolution (Å)	51.11-2.79	51.33-2.25
R_{sym}(%)[a]	8.3 (1.00)[b]	7.8 (56.3)
R_{pim} (%)	5.6 (67.6)	5.6 (45.3)
Overall $I/\sigma(I)$	8.4 (2.4)	8.0 (2.2)
#Unique Reflections	7609	13575
#Total Reflections	22238	36953
% Complete	92.9 (95.2)	94.3 (97.9)
CC(1/2)	0.997 (0.457)	0.992 (0.645)
Multiplicity	3.0 (3.5)	2.7 (2.3)
Refinement Statistics		
Resolution (Å)		51.33-2.25
R_{work}/R_{free}(%)[c]		21.4/24.6
Rmsd		
Bond angles (º)		0.687
Bond lengths (Å)		0.004
Ramachandran analysis		
Favored (%/)		98.04
Disallowed(%)		0.0

[a] $R_{sym} = \sum\sum|Ihkl-Ihkl(j)|/ \sum Ihkl$, where Ihkl(j) is observed intensity and Ihkl is the final average value of intensity. [b] values in parentheses are for the highest resolution shell. [c] $R_{work} = \sum||Fobs| - |Fcalc||/\sum|Fobs|$ and $R_{free} = \sum||Fobs| - |Fcalc||/\sum|Fobs|$; where all reflections belong to a test set of 5% randomly selected data.

Supplementary References

1. Bimboim, H.C., Doly, J., (1979). A rapid alkaline extraction procedure for screening recombinant plasmid DNA. *Nucleic. Acids. Res*. **7**, 1513-1523.
2. Sambrook, J., Russell, D.W., (2001). Molecular cloning: a laboratory manual, 3rd ed. Cold Spring Harbour Laboratory Press, Cold Spring Harbour, N. Y.
3. Brückner, R., (1992). A series of shuttle vectors for *Bacillus subtilis* and *Escherichia coli*. *Gene* **122**, 187-192.
4. Veiga, H., Jorge, A.M., Pinho, M.G., (2011). Absence of nucleoid occlusion effector Noc impairs formation of orthogonal FtsZ rings during *Staphylococcus aureus* cell division. *Mol. Microbiol*. **80**, 1366-1380.
5. Schumacher, M.A., Lee, J., Zeng, W., (2016). Molecular insights into DNA binding and anchoring by the *Bacillus subtilis* sporulation kinetochore-like RacA protein. *Nucl. Acids. Res.* **44**, 5438-5449.
6. Miroux, B., Walker, J.E., (1996). Over-production of proteins in *Escherichia coli*: mutant hosts that allow synthesis of some membrane proteins and globular proteins at high levels. *J. Mol. Biol*. **260**, 289-298.
7. Kreiswirth, B.N., et al., (1983). The toxic shock syndrome exotoxin structural gene is not detectably transmitted by a prophage. *Nature* **305**,709-712.
8. Lau, I.F., Filipe, S.R., Søballe, B., Økstad, O.A., Barre, F.X., Sherratt, D.J., (2003). Spatial and temporal organization of replicating *Escherichia coli* chromosomes. *Mol. Microbiol*. **49**,731-743.
9. Liew, A.T.F., et al., (2011). A simple plasmid-based system that allows rapid generation of tightly controlled gene expression in *Staphylococcus aureus*. *Microbiology* **157**,666-676.
10. Brückner, R., (1992). A series of shuttle vectors for *Bacillus subtilis* and *Escherichia coli*. *Gene*, **122**,187-192.
11. Jensen, S.O., Apisiridej, S., Kwong, S.M., Yang, Y.H., Skurray, R.A., Firth, N., (2010). Analysis of the prototypical *Staphylococcus aureus* multiresistance plasmid pSK1. *Plasmid* **64**,135-142.
12. Firth, N., et al., (2000). Replication of staphylococcal multiresistance plasmids. *J. Bacteriol.* **182**,2170-2178.
13. Brzoska, A.J., Firth, N., (2013). Two-plasmid vector system for independently controlled expression of green and red fluorescent fusion proteins in *Staphylococcus aureus*. *Appl. Environ. Microbiol.* **79**,3133-3136.